

The MOF-derived Cu₃P nanoparticles Coated in N-doped carbon nanosheets for Efficient Nitrogen Reduction Reaction

Jian Li, Xiaoying Lu, Junfeng Huang, Kailu Guo, Cailing Xu*

1. Experiment section

1.1 Chemicals

Copper(II) sulfate pentahydrate CuSO₄·5H₂O (KESHI, ≥99.0%), 4,5-imidazoledicarboxylic acid (aladdin, ≥97%), sodium hydroxide NaOH (Rionlon, ≥96%), Sodium sulfate anhydrous Na₂SO₄ (aladdin, ≥99%), Salicylic acid C₇H₆O₃ (Fengchuan, ≥99.5%), Sodium nitroprusside dihydrate Na₂[Fe(CN)₅NO]·2H₂O (Energy Chemical, ≥99%), sodium salicylate C₇H₅O₃Na (Kermel, ≥99.0%), Sodium hypochlorite solution (DAMAO, available chlorine ≥8%), ammonium chloride NH₄Cl (XL, ≥99.5%), Hydrazine hydrate N₂H₄·H₂O (DAMAO, ≥80%), 4-Dimethylaminobenzaldehyde C₉H₁₁NO (Alfa Aesar, ≥98%), Ethanol C₂H₆O (Rionlon, ≥99.7%), NaH₂PO₂·H₂O (Kermel, ≥98%). The deionized water (DI-water) was used throughout the synthesis.

1.2 Synthesis of materials

1.2.1 Preparation of Cu-MOFs

4,5-Imidazoledicarboxylic acid (1.2 mmol) was dispersed in 72 mL 0.02 M NaOH solution in a 150 mL breaker. CuSO₄·5H₂O (1.2 mmol) was dissolved in 24 mL DI-water and injected in the above solution. The mixed solution was stirred at room temperature for 3 h. The blue sediment was centrifuged, washed with DI-water and

ethanol for several times and dried at 60 °C for 12 h.

1.2.2 Preparation of Cu₃P@NC

50 mg of the above Cu-MOFs was placed in the porcelain boat at the downstream of the tubular furnace and 2.0 g of NaH₂PO₂·H₂O was placed in another porcelain at the upstream of the tubular furnace. Then, the tubular furnace was heated to 300 °C with 5 °C/min and kept for 2 h under the Ar flow.

1.2.3 Preparation of pure Cu₃P

100 mL 0.05 M CuSO₄ solution and 40 mL 0.25 M NaOH solution were mixed in a 150 mL breaker. Then, the above solution was stirred at room temperature for 2 h. After that, the blue sediment was centrifuged, washed with DI-water several times. Finally, the product and NaH₂PO₂·H₂O (mass ratio 1:5) were put into two different porcelain boat and annealed at 300 °C for 2 h with 5 °C/min under the Ar flow.

1.2.4 Preparation of pure Cu₃P@C

Synthesis of Cu₂O cubes: Typically, CuSO₄ (0.11 g) and PVP (0.2 g) were added to DI-water (17 mL) in a round-bottomed flask accompanied with magnetic stirring to achieve complete dissolution, denoted as solution A. Trisodium citrate dihydrate (0.22 g) and Na₂CO₃ (0.13 g) were dissolved in DI-water (2 mL), denoted as solution B. Then, the solution B was dropwise added into solution A at room temperature until the dark blue solution generated. After 20 min, glucose solution (2 mL, 0.6 M) was dropwise added into mixture at 80 °C. When the color of the suspension transformed darkblue into brick red, the mixture remained aged for 2 h. After cooling to room temperature naturally, the resulting precipitate was separated and collected by centrifugation for 5

min, followed by washing with DI-water and ethanol several times, respectively, and eventually dried in a vacuum at 60 °C for 12 h.

Synthesis of 3D Cu-BDC nanoarray (Cu-BDCNA): Cu₂O (10 mg) was dispersed in DMF (10 mL) with magnetic stirring to form solution C. H₂BDC (0.167 g) was completely dissolved in DMF (10 mL) to form solution D. Then, solution D was added into solution C under magnetic stirring at 120 °C. After continuous stirring for 10 min, the obtained mixed solution was aged at 120 °C for 1 h. The resulting precipitate was collected by centrifugation for 5 min, washed with DI-water and ethanol several times, respectively, and dried at 60 °C for overnight.

The Cu₃P@C catalysts were synthesized through phosphorization procedure using the as-prepared Cu-BDCNA as precursors. Typically, the as-prepared Cu-BDCNA and NaH₂PO₂ (*m/m* = 1/5) were placed at two separate positions in a quartz tube with NaH₂PO₂ at the upstream side. The quartz tube was thermally treated at a temperature of 350 °C with a ramp rate of 3 °C min⁻¹ and then maintained at this temperature for 5 h under a flowing Ar. After naturally cooling to room temperature, the obtained phosphatized catalyst was collected and washed with DI-water and ethanol for several times, respectively, and dried in an oven at 60 °C for 12 h.

1.3 The preparation of working electrode

Typically, 3 mg catalyst and 3 mg carbon black were dispersed in a mixed solution containing 40 μL Nafion solution and 730 μL ethyl alcohol and 730 μL DI-water. Next, the mixed solution was sonicated for 1 h to form a homogeneous ink. Then, 100 μL of the above ink was dropped on the carbon cloth with area 1 × 1 cm².

1.4 Characterizations

The powder X-ray diffraction (XRD) pattern were measured on a Rigaku D/max 2400 X-ray generator diffractometer. Scanning electron microscopy (SEM) was performed on a Thermo Scientific Apreo S machine. Transmission electron microscope (TEM) images and energy dispersive X-ray spectroscopy (EDS) mapping were obtained from a transmission electron microscope (Philips Tecnai™ G2 F30). High-angle annular dark-field scanning transmission electron microscopy (HAADF-STEM) images were acquired on an aberration-corrected TEM (Titan Themis Cubed G2 300) operated at 300 kV. The UV-vis absorption spectra were observed on a Cary-5000 spectrophotometer. Fourier transform infrared spectroscopy spectra (FTIR) were collected by a Bruker VERTEX 70v FT-IR spectrometer. X-ray photoelectron spectroscopy (XPS) measurements were performed on a PHI-5702 instrument operated with a Mg-K α excitation source (1253.6 eV). Binding energies (BE) were determined using the C 1s peak at 284.8 eV as a charge reference. Thermogravimetric (TG) analysis was conducted on Netzsch STA 449C, with a heating rate of 5 °C min⁻¹ from 25 to 750 °C under highly pure N₂ atmosphere. The absorbance data of the ultraviolet-visible (UV-vis) spectrophotometer was measured on an Agilent Cary 5000. Raman spectra measurements were carried out on a Raman spectrometer (Jobin Yvon Co., France) model HR800 and 532 nm laser as the excitation wavelength.

1.5 Electrochemical measurement

The electrochemical experiment was carried out with an Autolab electrochemical workstation (PGSTAT302N, Metrohm) in a two-compartment electrolytic cell

containing 50 mL 0.1 M Na₂SO₄ solution. The standardized three-electrode configuration includes Cu₃P@NC/CP as working electrode, carbon rod as counter electrode and Ag/AgCl as reference electrode, respectively. The potentials with respect to reversible hydrogen electrode is calculated by the following equation, E(vs. RHE) = E(vs. Ag/AgCl) + 0.059 × pH + 0.197 V. Before NRR measurement, 0.1 M Na₂SO₄ solution electrolyte was purged with pure N₂ for 30 min. All experiments were operated at room temperature.

1.6 Determination of NH₃

The ammonia produced by electrochemical NRR was detected via UV-vis spectrophotometer using indophenol blue method¹. Typically, 2 mL of electrolyte was taken out from the cathodic cell after 2 h NRR process. Then, 2 mL of NaOH solution composed of 5 wt% sodium citrate and 5 wt% salicylic acid, 1 mL of 0.05 M NaClO solution and 0.2 mL wt% sodium nitroprusside dihydrate was added into the above electrolyte in turn. After the mixed solution was kept in the dark for 2 h, the UV-vis spectrophotometer was used to measure the wavelength at 655 nm. The concentration-absorbance curve was calibrated using standard NH₄Cl solution with a series of concentrations. The fitting curve ($y = 0.571x + 0.0465$, $R^2 = 0.999$) shows good linear relation of absorbance value with NH₃ concentration. The produced NH₃ yield rate was calculated by the following equation:

$$NH_3 \text{ Yield Rate} = \frac{[NH_3] \times V}{m_{cat.} \times t}$$

Where [NH₃] is the produced NH₃ concentration (μg mL⁻¹), V is the volume of electrolyte (mL), t is the NRR time (min) and m_{cat.} is the loaded mass of catalyst (mg).

1.7 Calculation of Faradaic efficiency (FE):

FE was calculated according to the following equation:

$$FE = \frac{3 \times F \times [NH_3] \times V}{Q \times 17}$$

Where $[NH_3]$ is the produced NH_3 concentration ($\mu g mL^{-1}$), V is the volume of electrolyte (mL), F is the Faradaic constant, Q is the quantity of charge in Coulombs (C).

1.8 Determination of N_2H_4

The possible by-product N_2H_4 was determined via Watt and Chrisp method². The color agent was prepared with 5.99 g of p-Dimethylaminobenzaldehyde, 30 mL of concentrated hydrochloric acid and 300 mL of ethanol. In detail, 5 mL of electrolyte was removed from the cathodic cell after 2 h NRR. Then, 5 mL of color agent was added to the above electrolyte. After standing in the dark for 20 minutes, the solution was measured on a UV-vis spectrophotometer. The maximum UV-vis absorption was measured at 455 nm. The concentration-absorbance curves were calibrated using standard $N_2H_4 \cdot H_2O$ solution in a series of concentration. The fitting curve ($y = 0.613x + 0.014$, $R^2 = 0.999$) shows a good linear relation between absorbance with N_2H_4 concentration.

2. Figures

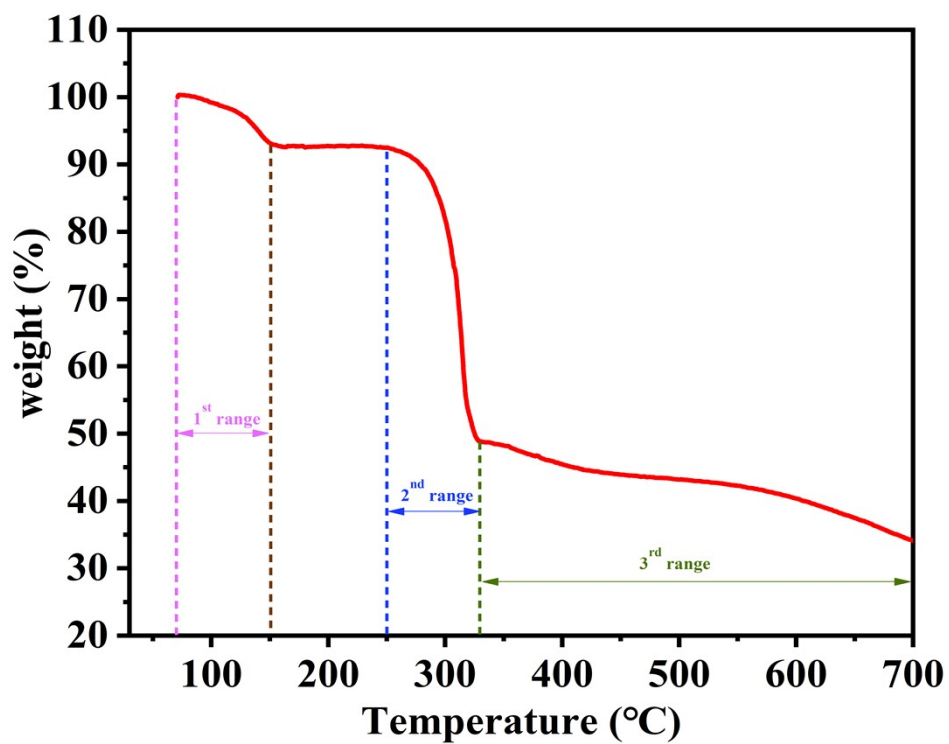


Fig. S1. The TG curve of synthesized Cu-MOFs.

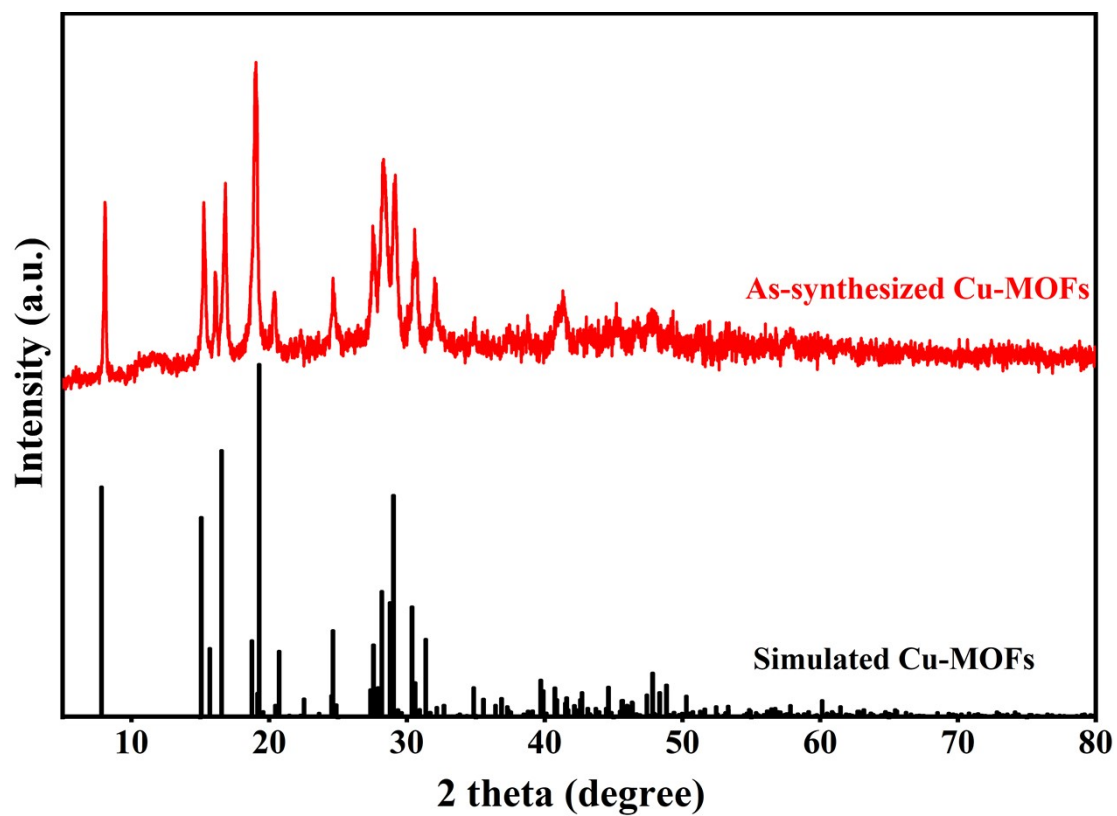


Fig. S2. The XRD patterns of synthesized Cu-MOFs.

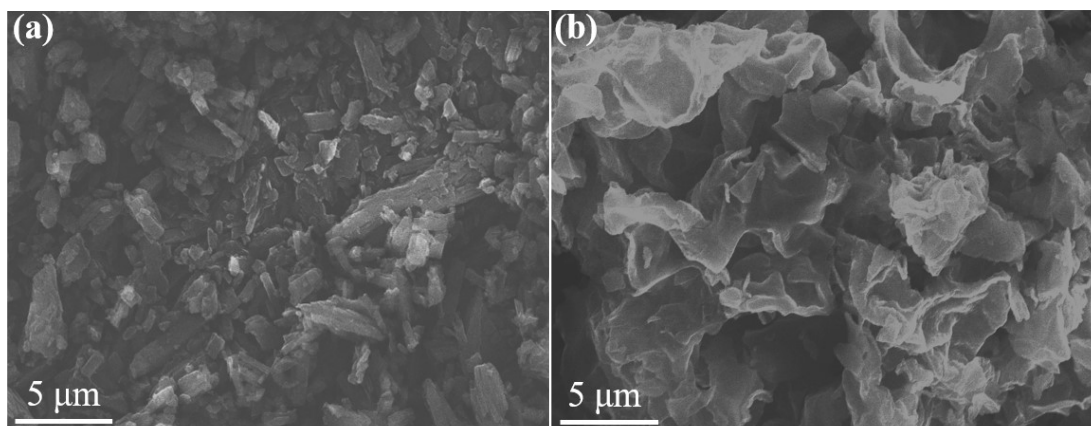


Fig. S3. The SEM image of synthesized (a) Cu-MOFs and (b) Cu₃P@NC .

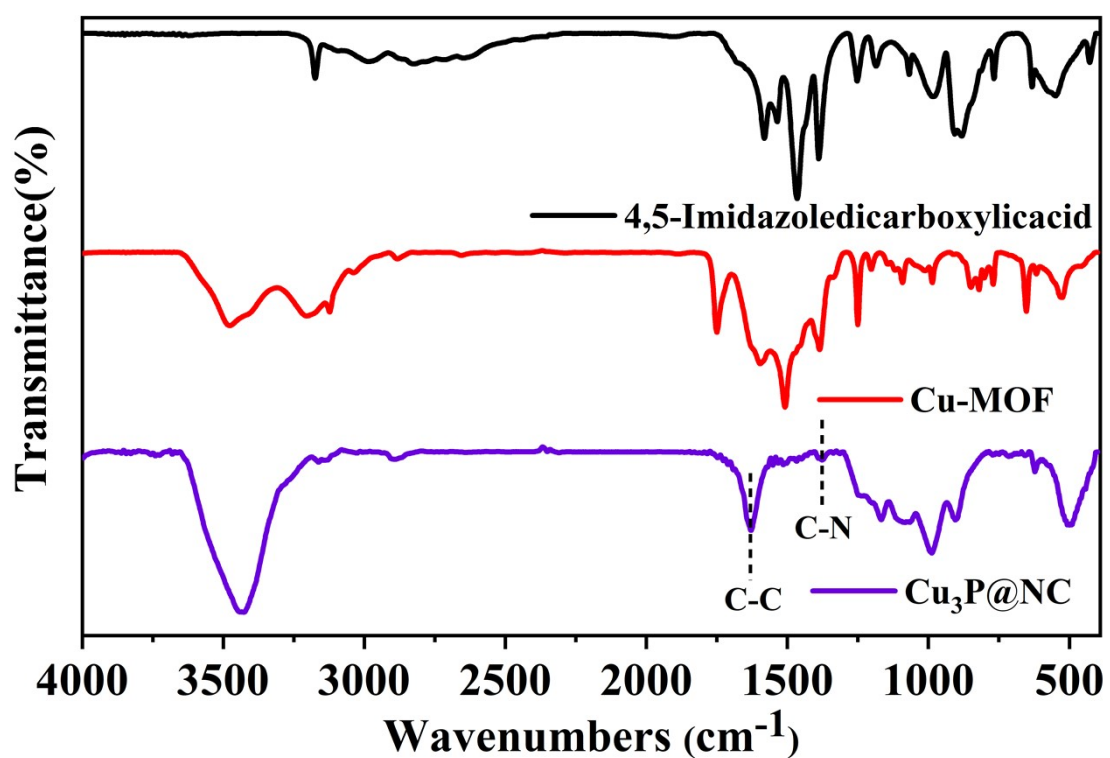


Fig. S4. The FT-IR spectra of 4,5-imidazoledicarboxylic acid, Cu-MOFs and Cu₃P@NC.

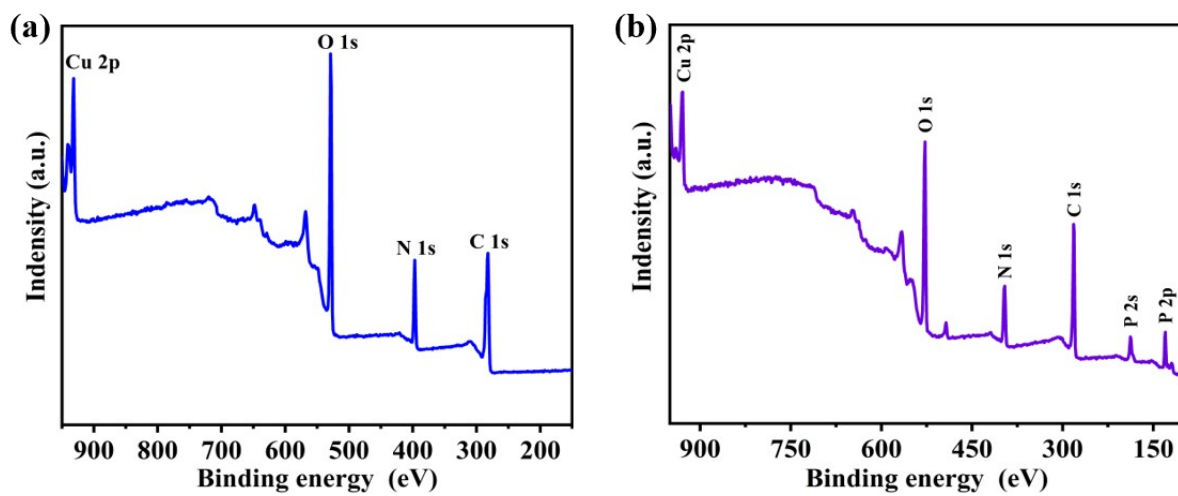


Fig. S5. XPS spectra of (a) Cu-MOFs and (b) Cu₃P@NC.

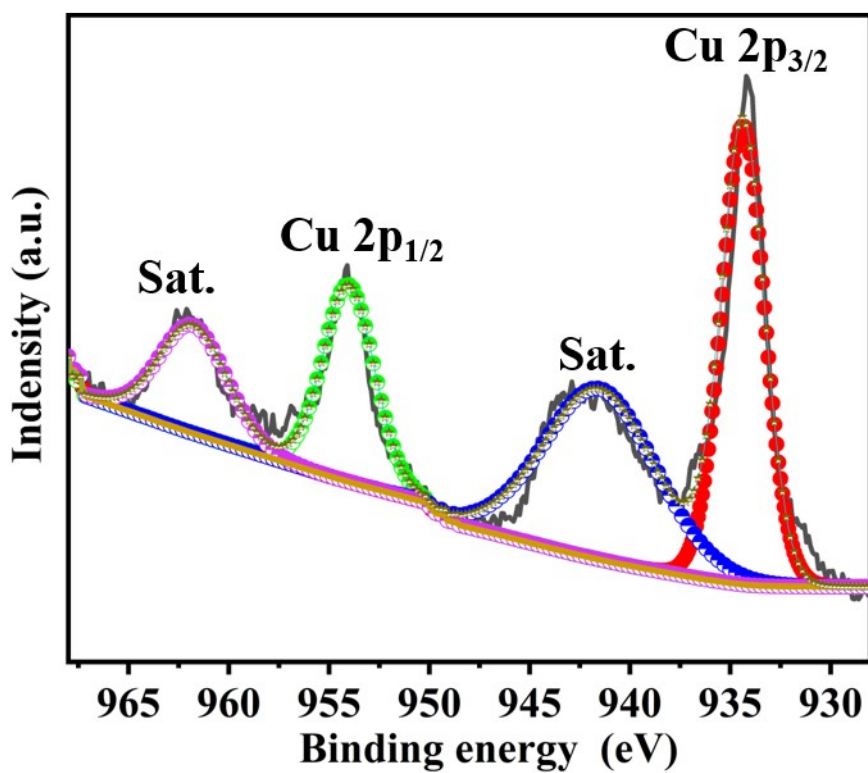


Fig. S6. The high-resolution Cu 2p XPS spectra of pristine Cu-MOFs.

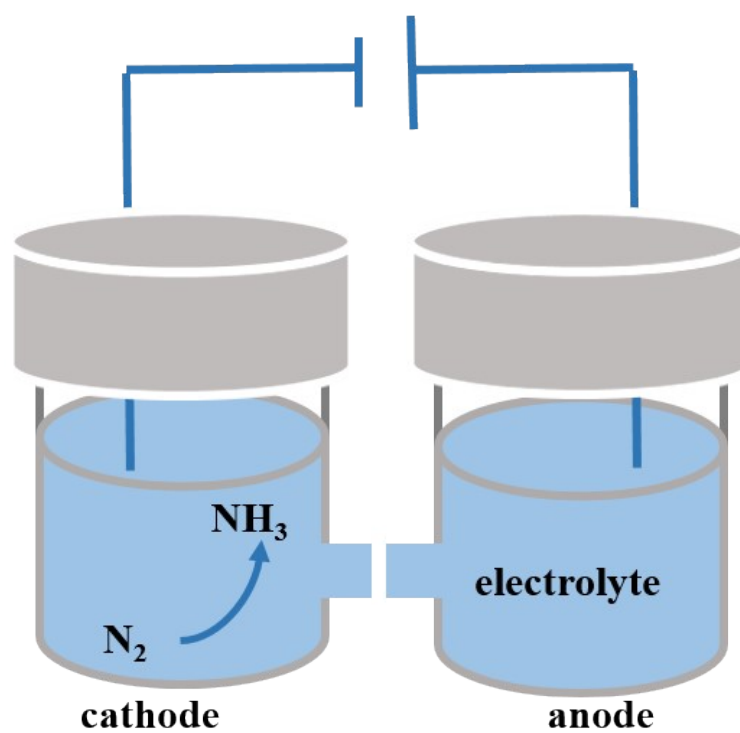


Fig. S7. The simple schematic diagram of H-type cell.

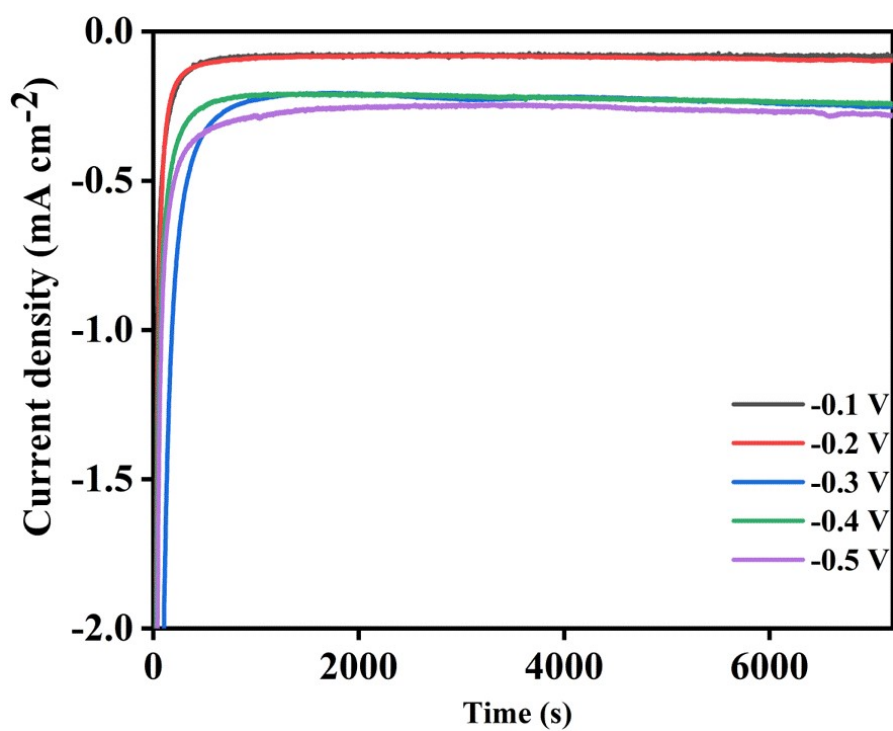


Fig. S8. Chronoamperometry results of $\text{Cu}_3\text{P@NC}$ at the corresponding potentials.

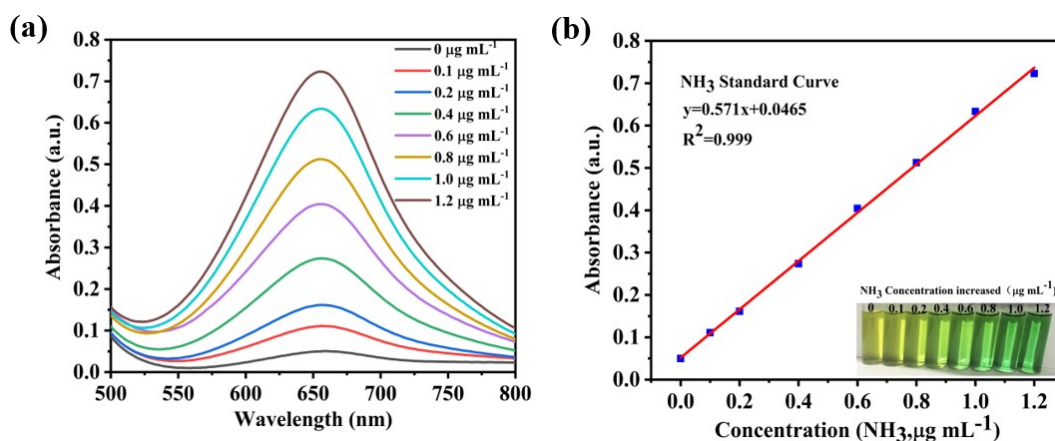


Fig. S9. UV-vis absorption spectra of indophenol assays with NH_4^+ in 0.1 M Na_2SO_4 after incubated for 2 h at room temperature. (b) Calibration curve used for calculation of NH_3 concentration.

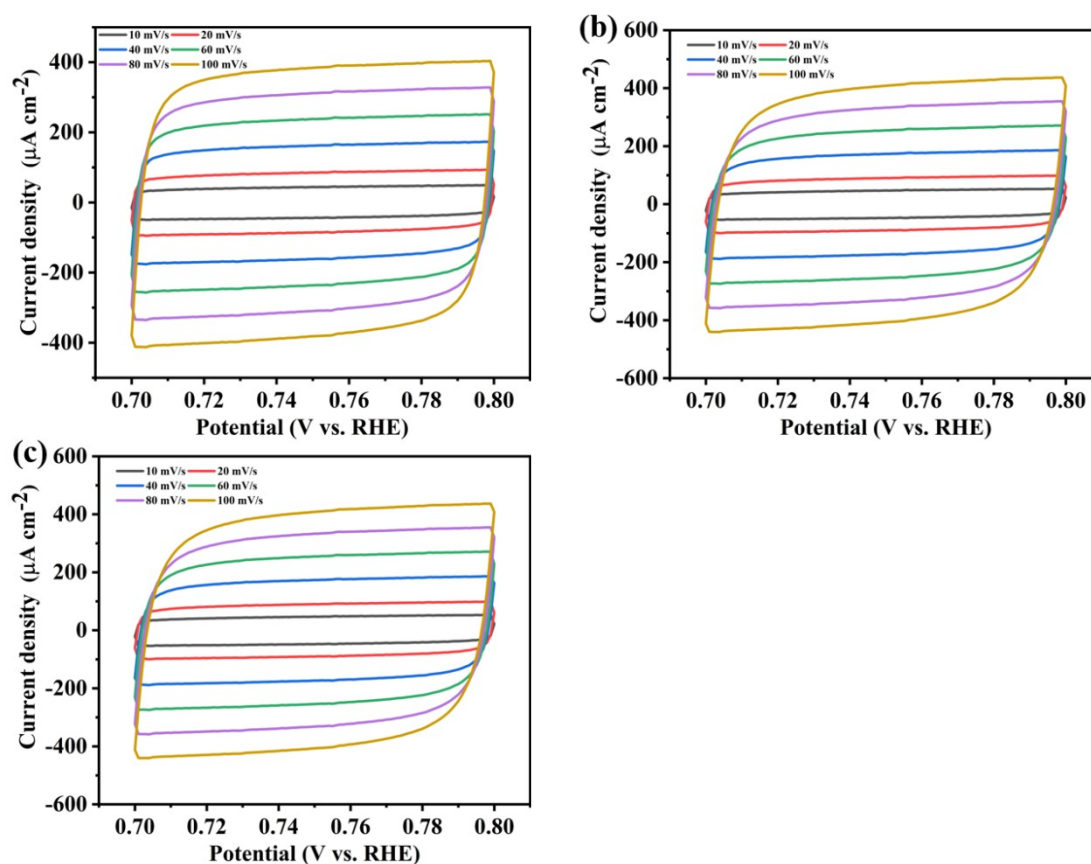


Fig. S10. The CV curves of (a) Cu_3P , (b) $\text{Cu}_3\text{P}@C$ and (c) $\text{Cu}_3\text{P}@NC$ at different scan rates.

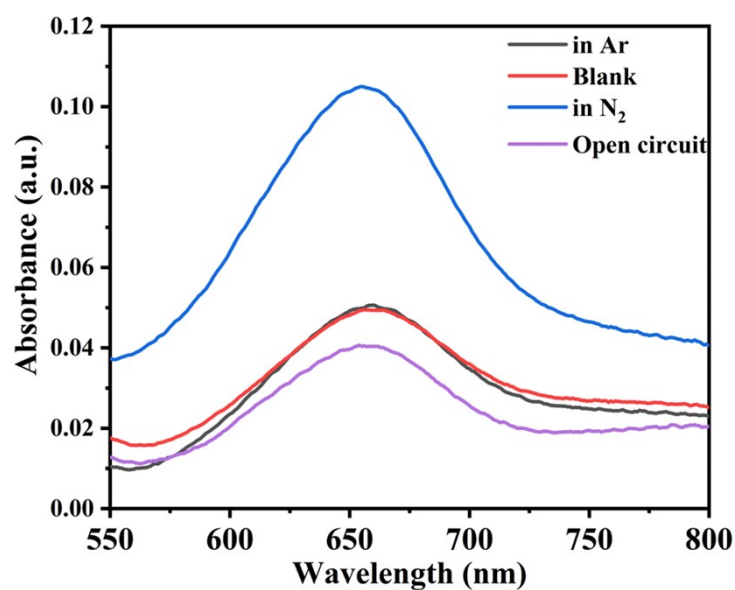


Fig. S11. UV-vis absorption spectrums of all controlled experiments including Ar gas, blank carbon and open circuit.

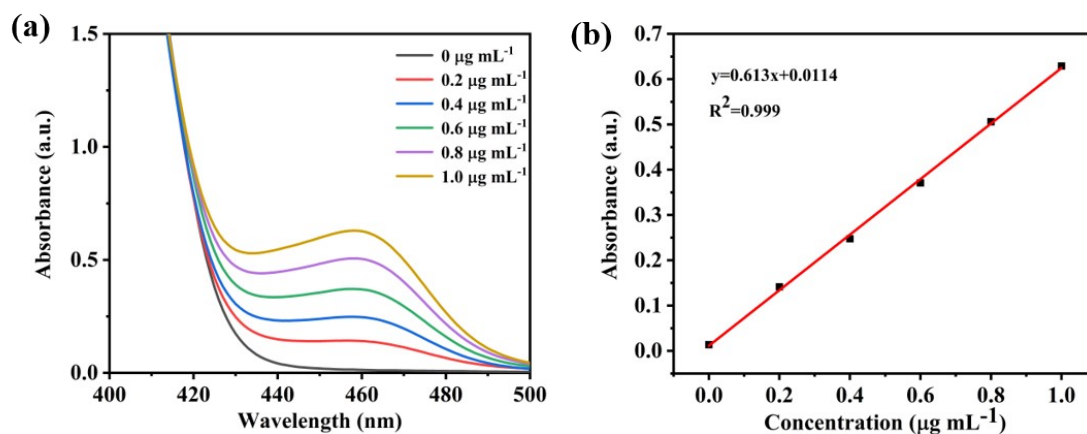


Fig. S12. UV-vis absorption spectra of various N_2H_4 concentration stained with p- $C_9H_{11}NO$ indicator after incubated for 20 min at room temperature. (b) Calibration curve used for calculation of N_2H_4 concentration.

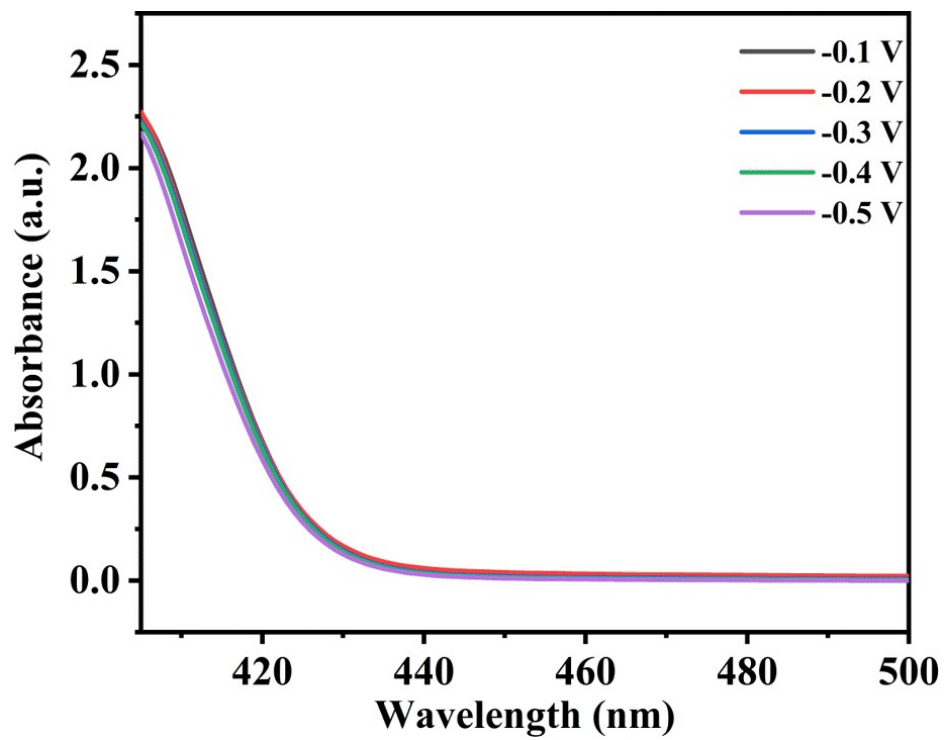


Fig. S13. UV-vis absorption spectra Cu₃P@NC of at corresponding potentials to detect by-product.

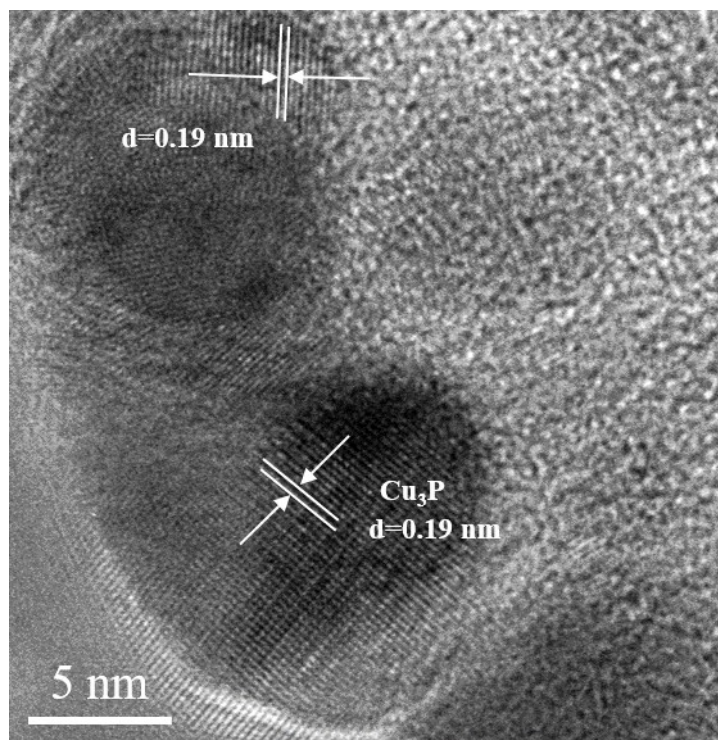


Fig. S14. High-resolution TEM image of the Cu₃P@NC after NRR test.

Table S1. Comparison of the NRR activity of the Cu₃P@NC with other electrocatalysts previously reported.

Catalysts	Electrolytes	NH ₃ yield rate	FE (%)	Reference
ZrO ₂	0.1 M Na ₂ SO ₄	9.6 μg h ⁻¹ mg ⁻¹	12.1	3
Fe-MoS ₂	0.5 M K ₂ SO ₄	8.6 μg h ⁻¹ mg ⁻¹	18.8	4
Pd/C	0.1 M PBS	4.5 μg h ⁻¹ mg ⁻¹	8.2	5
Pd-Co/CuO	0.1 M KOH	10.04 μg h ⁻¹ mg ⁻¹	2.16	6
PdCu Amorphous Nanocluster	0.1 M KOH	2.8 μg h ⁻¹ mg ⁻¹	0.38	7
Au nanorods	0.1 M KOH	6.042 μg h ⁻¹ mg ⁻¹	4	8
SnO ₂	0.1 M Na ₂ SO ₄	4.03 μg h ⁻¹ mg ⁻¹	2.17	9
PdZn/NHCP	0.1 M PMS	5.3 μg h ⁻¹ mg ⁻¹	16.9	10
γ-Fe ₂ O ₃	0.1 M KOH	0.212 μg h ⁻¹ mg ⁻¹	1.9	11
aAu/CeOxRGO	0.1 M HCl	8.3 μg h ⁻¹ mg ⁻¹	10.1	12
BCN	0.1 M HCl	7.75 μg h ⁻¹ mg ⁻¹	13.79	13
Cu₃P@NC	0.1 M Na₂SO₄	10.4 μg h⁻¹ mg_{cat.}⁻¹	6.34	This work

Reference:

1. Ying Wang, Xiaoqiang Cui, Jingxiang Zhao, Guangri Jia, Lin Gu, Qinghua Zhang, Lingkun Meng, Zhan Shi, Lirong Zheng, Chunyu Wang, Ziwei Zhang,[†] and Weitao Zheng, *ACS Catal.* 2019, 9, 336-344.
2. Jiaxin Yao, Yitong Zhou, Jun-Min Yan, and Qing Jiang, *Adv. Energy Mater.* 2021, 2003701.
3. Jiaojiao Xia, Haoran Guo, Maozeng Cheng, Chuyan Chen, Minkang Wang, Yong Xiang, a Tingshuai Li and Enrico Traversa, *J. Mater. Chem. A*, 2021,9, 2145-2151.
4. Hongyang Su, Lanlan Chen, Yizhen Chen, Rui Si, Yuting Wu, Xiaonan Wu, Zhigang Geng, Wenhua Zhang, and Jie Zeng, *Angew. Chem.* 2020, 132, 20591 –20596.
5. Jun Wang, Liang Yu, Lin Hu, Gang Chen, Hongliang Xin, Xiaofeng Feng, *Nature communications* | (2018) 9:1795.
6. Wenzhi Fu, Yudong Cao, Qianyi Feng, William R. Smith, Pei Dong, Mingxin Ye and Jianfeng Shen, *Nanoscale*, 2019, 11, 1379–1385.
7. Shi, M. M.; Bao, D.; Li, S. J.; Wulan, B. R.; Yan, J. M.; Jiang, Q. J. A. E. M., *Adv. Energy Mater.* 2018, 8 (21), 1800124.
8. Bao, D.; Zhang, Q.; Meng, F. L.; Zhong, H. X.; Shi, M. M.; Zhang, Y.; Yan, J. M.; Jiang, Q.; Zhang, X. B. J. A. m, *Adv. Mater.* 2017, 29 (3), 1604799.
9. Zhang, L.; Ren, X.; Luo, Y.; Shi, X.; Asiri, A. M.; Li, T.; Sun, X., *Chem. Commun.* 2018, 54, 12966–12969.
10. Min Ma, Xiao Han, Huiqi Li, Xibo Zhang, Zhiping Zheng, Lingyun Zhou, Jun Zheng, Zhaoxiong Xie, Qin Kuan, Lansun Zheng, *Applied Catalysis B: Environmental*

265 (2020) 118568.

11. Kong, J.; Lim, A.; Yoon, C.; Jang, J. H.; Ham, H. C.; Han, J.; Nam, S.; Kim, D.; Sung, Y.-E.; Choi, J. J. A. S. C, ACS Sustain. Chem. Eng. 2017, 5 (11), 10986-10995.

12. Li, S. J.; Bao, D.; Shi, M. M.; Wulan, B. R.; Yan, J. M.; Jiang, Q, Adv. Mater. 2017, 29, 1700001.

13. Chen, C.; Yan, D.; Wang, Y.; Zhou, Y.; Zou, Y.; Li, Y.; Wang, S, Small 2019, 15,1805029.

